

Inhibitory Effects of Anti-VEGF Antibody on the Growth and Angiogenesis of Estrogen-induced Pituitary Prolactinoma in Fischer 344 Rats: Animal Model of VEGF-targeted Therapy for Human Endocrine Tumors

Katsuhiko Miyajima^{1,3}, Susumu Takekoshi¹, Johbu Itoh², Kochi Kakimoto^{1,3}, Takashi Miyakoshi¹ and Robert Yoshiyuki Osamura¹

¹Department of Pathology, Tokai University School of Medicine, 143 Shimokasuya, Isehara, Kanagawa 259–1193, Japan,

²Teaching and Research Support Center, Tokai University School of Medicine, 143 Shimokasuya, Isehara, Kanagawa 259–1193, Japan and ³Japan Tobacco Inc., Toxicology Research Laboratories, Central Pharmaceutical Research Institute, 23 Nagasaki, Hadano, Kanagawa 257–0024, Japan

Received October 14, 2009; accepted November 3, 2009; published online April 7, 2010

Estrogen-induced pituitary prolactin-producing tumors (PRLoma) in F344 rats express a high level of vascular endothelial growth factor (VEGF) associated with marked angiogenesis and angiectasis. To investigate whether tumor development in E2-induced PRLoma is inhibited by anti-VEGF monoclonal antibody (G6-31), we evaluated tumor growth and observed the vascular structures. With simultaneous treatment with G6-31 for the latter three weeks of the 13-week period of E2 stimulation (E2+G6-31 group), the following inhibitory effects on the PRLoma were observed in the E2+G6-31 group as compared with the E2-only group. In the E2+G6-31 group, a tendency to reduction in pituitary weight was observed and significant differences were observed as (1) reductions in the Ki-67-positive anterior cells, (2) increases in TUNEL-positive anterior cells, and (3) repair of the microvessel count by CD34-immunohistochemistry. The characteristic “blood lakes” in PRLomas were improved and replaced by repaired microvascular structures on 3D observation using confocal laser scanning microscope. These inhibitory effects due to anti-VEGF antibody might be related to the autocrine/paracrine action of VEGF on the tumor cells, because VEGF and its receptor are co-expressed on the tumor cells. Thus, our results demonstrate that anti-VEGF antibody exerted inhibitory effects on pituitary tumorigenesis in well-established E2 induced PRLomas.

Key words: anti-VEGF antibody, VEGF, estrogen, prolactinoma, angiogenesis

I. Introduction

Estrogen is known to be the most important hormone for the regulation of physiologic development and cell proliferation, and has been implicated in the pathogenesis of endocrine lesions and several types of cancers [24, 37, 46]. Estrogen can also induce tumors in a variety of animal models, among which prolactin-producing pituitary tumors (PRLoma) can be induced in Fischer 344 (F344) rats by long-term estradiol (E2) treatment [34, 44, 47]. The mech-

anism by which estrogenic-agents act to promote PRL cell proliferation and angiogenesis is not fully understood. However, recent reports have indicated that several hormones and growth factors including VEGF are expressed in the anterior pituitary [6, 8, 45] and furthermore the disruption of dopaminergic regulation could result in the progression of PRLoma with abnormal pituitary blood flow and drastic changes in the anterior pituitary vasculature [9, 10, 20, 29]. Angiogenesis is an important factor for tumor growth [21] and abnormal tumor-related vasculature has been an effective target for anticancer therapy [12, 16, 17]. Considering the relevance of angiogenesis in tumor development, it is expected that tumor growth could be blocked by anti-angiogenic agents [49, 50], and the use of

Correspondence to: Robert Yoshiyuki Osamura, M.D., Ph.D., Department of Pathology, Tokai University School of Medicine, 143 Shimokasuya, Isehara, Kanagawa 259–1193, Japan.
E-mail: osamura@is.icc.u-tokai.ac.jp

anti-VEGF agents to prevent tumorigenesis would introduce a beneficial therapy for vascular abundant endocrine tumors. Among the many angiogenic growth factors involved, VEGF appears to play an important role in the formation of the vascularity originally found in pituitary cells [11], among which subtype VEGF-A is the most important member in the VEGF family in stimulating peripheral circulatory permeability [13]. VEGF has also been demonstrated to be involved in mediation of the proliferative effect on the PRL cells by estrogenic action [43]. In addition, estrogen stimulates VEGF synthesis in the tumor cells and increased tumoral VEGF production was enhanced during the progress of E2-induced PRLoma [1, 2]. Flk-1 (known as VEGF receptor-2) has been shown to be expressed in endothelial cells and also is found to mediate the function of mitogenesis on VEGF stimulation [53]. Furthermore, dominant-negative inhibition of Flk-1 has been found to reduce tumor angiogenesis and growth [38] and these findings suggest that Flk-1 plays an important role in the development of tumor angiogenesis and growth [54]. Expression of Flk-1 has been reported to be detected in the anterior pituitary cells and this finding supports the autocrine/paracrine functions of VEGF in the rat pituitary cells [1, 53]. Increased expression levels of VEGF and Flk-1 have been reported in the peripheral blood of patients with pituitary tumors [30].

Anti-VEGF antibody (bevacizumab, Genentech Inc.) is a therapeutic agent designed to inhibit tumor angiogenesis in human cancers. The G6-31 (Anti-VEGF antibody: kindly supplied by Genentech Inc.) used in this study has been confirmed to bind to both human and murine VEGF. The nature of this antibody is known to be related to bevacizumab therapy [19, 33] and this antibody has been shown to inhibit the binding of human and murine VEGF to VEGF-receptors *in vitro* and has also been shown to be effective against rat VEGF [33]. Liang *et al.* reported that anti-VEGF antibody could reduce tumor volume in xenografts in SCID mouse after stimulation with G6-31 [33], and Korsisaari *et al.* has reported the results of injection of G6-31 into the Apc+/*min* line of mice, which are susceptible to developing intestinal adenomas suppression [31]. Also, in the endocrine system, inhibition of the growth of pituitary adenoma and reduction in serum prolactin levels by G6-31 has been reported in the MEN1 mouse model [32].

The aim of this study is to elucidate the inhibitory effects of G6-31 on the development and angiogenesis of well-established E2-induced PRLoma. Our data suggested that blocking of VEGF-A by G6-31 could indicate a strategy to inhibit tumor growth not only by inhibition of angiogenesis-dependent tumor growth, but also by inhibiting PRL cell proliferation and enhancing apoptosis directly associated with the autocrine/paracrine action of VEGF produced by the tumor cells.

II. Materials and Methods

Animals

Female Fischer 344 rats, 6-wks of age, were purchased

from Charles River Co. (Kanagawa, Japan), and kept in stainless steel bracket cages under 12-h light/dark (lights on from 7 a.m. to 7 p.m.) and temperature (20–25°C). The animals were maintained in animal care facilities, with water and food supplied *ad libitum*. This experiment was conducted under guidelines for the use and care of laboratory animals, approved by the institutional animal care committee of Tokai University.

Study design

The study design is shown in Figure 1. Thirty-six animals were randomly allocated to three groups based on the body weights at 7 weeks of age, and each group consisted of 12 rats. Two groups rats were injected with 3000 µg/kg of estradiol (E2; estradiol dipropionate: Ovahormone Depot[®], ASKA Pharmaceutical Co., Ltd. Tokyo, Japan), once a week intramuscularly (i.m.) for 13 wks. After 10 wks of E2 dosing, one group (the E2+G6-31 group, n=12) was also injected intravenously (i.v.) with 5 mg/kg of G6-31 (anti-human and murine VEGF-A monoclonal antibody, kindly supplied by Genentech Inc., South San Francisco, CA, USA), once a week at 2 days after each E2 injection during the last 3 wks of the 13 wk-dosing period; and the other (E2 group, n=12) received saline (Otsuka Pharmaceutical Inc., Tokushima, Japan) in the same manner as the G6-31 treated group. For the vehicle control group (n=12), age and lot-matched female F344 rats were injected with sesame oil (Sigma-Aldrich, Inc., St Louis, MO, USA) intramuscularly instead of E2 together with saline intravenously in the same manner as the G6-31 treatment (Fig. 1).

Anti-VEGF antibody (G6-31)

Anti-human and murine VEGF-A monoclonal antibody (G6-31, Lot No. 11037) was kindly supplied by Genentech Inc., South San Francisco, CA, USA. The antibody is monoclonal antibody which reportedly binds to human and murine VEGF-A with high affinity [19].

Tissue preparation

Pituitaries from 6 rats in each group were used for histological observation and gene expression analysis while the remaining rats in each group (n=6) were used for three-dimensional (3D) imaging analysis of the tumor angiogenesis associated with tumor development by infusing FITC-conjugated gelatin into the anterior pituitary vessels.

The animals were sacrificed following 13 wks dosing with E2. Six rats were dissected in each group and their pituitaries were collected and weighed. For gene expression analysis small pieces were obtained from a consistent area in each anterior pituitary. Most of the pituitary tissues from each animal were fixed in 4% paraformaldehyde (0.1 M phosphate buffer, pH 7.4) for histological analysis and immunohistochemical procedures. For histological analysis, the fixed tissues were dehydrated and embedded in paraffin wax, sectioned at 4 µm thickness, and stained with H&E following standard protocols.

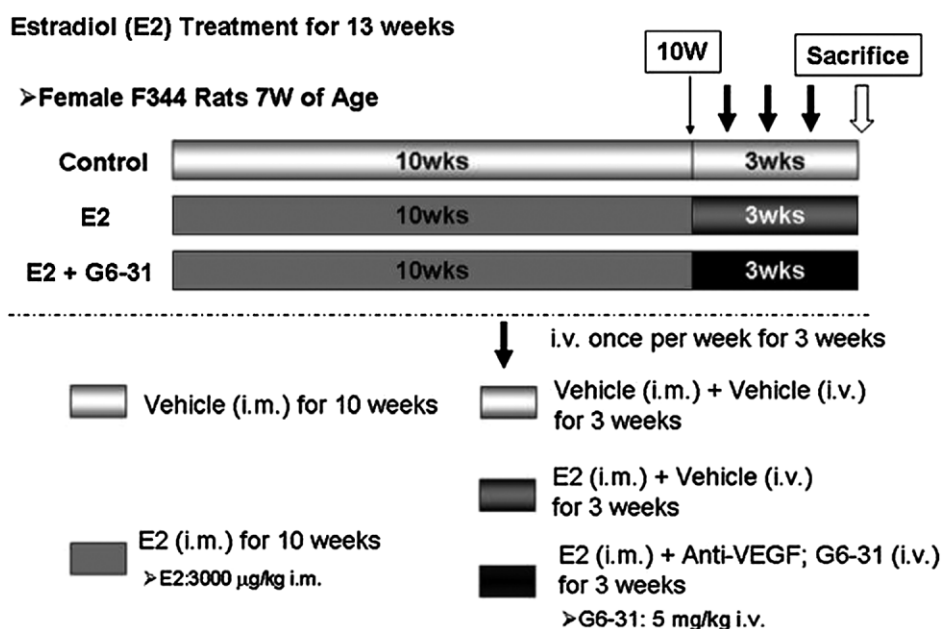


Fig. 1. Effect of G6-31 (Anti-VEGF-A antibody) on E2 induced pituitary PRLoma in female F344 rats. E2 group: treatment protocol for E2-induced PRLoma, at seven-week of age female rats were given E2 (i.m., once weekly) for 13 wks. E2+G6-31 group: In the same manner as the E2 group and during the last 3 wks of E2 dosing, simultaneous use of G6-31 (i.v., once weekly) for 3 wks. Control group: Animals were treated with sesame oil as with E2 and saline with G6-31. Details are provided in Materials and Methods.

Immunohistochemistry

For the immunohistochemical studies antibodies were purchased and diluted as follows: anti-VEGF antibody (A-20, Santa Cruz Biotechnology Inc., Santa Cruz, CA, USA, 1:50), anti-rPRL antibody (Chemicon, Millipore Corp., Billerica, MA, USA, 1:100), anti-Ki-67 antibody (MM-1, Novocastra Laboratories Ltd., Newcastle upon Tyne, UK, 1:80), and anti-hypoxia inducible factor-1 α antibody (HIF-1 α , Novus Biologicals, Littleton, CO, USA, 1:50), anti-Pituitary Tumor Transforming Gene antibody (PTTG-1, Zymed Laboratories, Inc., South San Francisco, CA, USA, 1:50), anti-CD34 antibody (C-18, sc-7045, Santa Cruz Biotechnology Inc., 1:80) and anti-VEGFR-2 antibody (KDR/Flk-1, A-3, Santa Cruz Biotechnology Inc., 1:50). For VEGF, rPRL, Ki-67 and HIF-1 α , staining was performed using Histofine Simple Stain Rat MAX PO for the rat tissue specific Simple Stain Rat MAX-PO MULTI (Nichirei Biosciences Inc., Tokyo, Japan), while that for PTTG, CD34 and VEGFR-2 was performed using CSA kit (Dako, Grostrup, Denmark) according to the manufacturer's instructions in the staining kits respectively. Sections were deparaffinized before quenching of endogenous peroxidase activity and blocking of endogenous biotin, and then put in a microwave oven in citrate buffer (pH 6.0) twice for 10 min and left to cool at room temperature. Sections were incubated with primary antibodies overnight at 4°C and each antibody was used at an appropriate concentration as described above. After incubation of the primary antibodies and using a detection kit, the sections were incubated in 3'3'-diaminobenzidine solution (Wako Pure Chemical Industries, Ltd.,

Osaka, Japan) as a chromogen, usually for 3 min. Sections were counter-stained lightly with hematoxylin.

Quantitative analysis of CD34-positive microvessels in the anterior pituitary

To evaluate the development of tumor angiogenesis in the anterior pituitary, immunohistochemical examination for CD34 was performed. Quantitation of the microvessels was carried out according to the methods previously reported [3, 4, 18]. To determine the microvascular density, sections immunostained for CD34 were first scanned under low magnification ($\times 40$) for hot spot areas (most dense vascular staining). Microvascular density was then determined by averaging the number of blood vessels in CD34-positive vessels in 10 fields selected at $\times 400$ magnification randomly in each of the pituitary slides. Mean numbers per field were calculated. The blood vessels were then classified into two categories according to their size (i.e. small and large). Blood vessels $< 5 \mu\text{m}$ were classified as small vessels and > 5 to $10 \mu\text{m}$ were classified as large vessels. Cystic blood lakes which were not lined by CD34-positive endothelial cells were also counted in the same manner.

Cell proliferation

Cell proliferation in the pituitary anterior was detected by immunohistochemical staining with Ki-67. Ki-67-positive nuclei were counted randomly from 1000 anterior pituitary cells in each rat pituitary in microscopic fields at $\times 400$ magnification in each section by blinded observation.

Determination of apoptosis

The number of apoptotic bodies was determined with the use of the terminal deoxynucleotidyltransferase (TdT)-mediated dUTP nick-end labeling (TUNEL) method. An *in situ* cell death detection kit (Apomark, Exalpa Biological, Inc., Boston, MA, USA) was used according to the manufacturer's instructions. The number of apoptotic cells was counted randomly per 2000 anterior pituitary cells in microscopic fields at $\times 400$ magnification in each section by blinded observation.

Three dimension imaging analysis of pituitary vessels

Three dimensional (3D) imaging observation of the anterior pituitary microvessels was conducted using the fluorescein-5-isothiocyanate (FITC) conjugate gelatin method [26]. For preparation of the FITC-gelatin conjugate, the use of fluorescent dye conjugated-polypeptide was introduced using acrylamide slab gels [51]. The high molecular weight fluorescein-labeled dextran methods were also reported [7]. We combined and modified these methods. Ten mg of FITC (Dojindo Laboratories, Kumamoto, Japan) was dissolved in 1 ml dimethylsulfoxide (DMSO; Sigma-Aldrich, Inc., St Louis, MO, USA) and mixed for conjugation to 20% gelatin (Sigma-Aldrich, Inc.) solution of pH 11 at 37°C for overnight. The FITC-conjugated gelatin (FITC-gelatin) was then dialyzed in 0.01 M phosphate buffered saline (PBS, pH 7.4) at 37°C in the dark for 1 week. One hundred ml of the FITC-gelatin solution was used for injection into each rat.

To demonstrate 3D images of the intrapituitary microvessels using the confocal laser scanning microscopy system (CLSM; LSM510-Meta, Carl Zeiss MicroImaging GmbH, Jena, Germany), FITC-gelatin solution was infused intravenously to six rats in each group. The abdominal and thoracic cavities of the rats were dissected under diethyl ether inhalation anesthesia. The rats were perfused with 0.1 M PBS from the left ventricle of the heart and the right atrium was excised to draw off the circulated fluid. After complete perfusion with PBS solution, FITC-gelatin solution was injected into the left ventricle of the heart for approximately up to 5 min through the systemic circulation from left ventricle. After infusion of 100 ml of FITC-gelatin solution, the rats were immediately cooled to coagulate the injected FITC-gelatin in the microvessels for 5 min and then the wet pituitary glands were removed and immediately fixed in graded cold 4% paraformaldehyde (PFA) overnight (4°C). The anterior pituitary tissues were cut into 2 mm cube blocks, placed on 50 \times 70-mm coverslips (Matsunami Glass, Osaka, Japan), and mounted in 0.05 M Tris-HCl buffer. Three dimensional images of the intrapituitary microvessels were observed by using the CLSM. The optical tomographic imaging (Z-images) for 3D reconstruction of the microvessels was conducted using a Plan-Apochromat ($\times 63$, water immersion, NA 1.25; Carl Zeiss MicroImaging) and Plan-Neofluar ($\times 10$, NA 0.30; $\times 20$, NA 0.50; Carl Zeiss MicroImaging) objective lens. Z-directional movement for the optical sectioning of the entire specimens was controlled

by a stepping motor unit for axial scanning at 0.5–20- μ m focus steps and in total the focus depth was about 200 μ m thickness for the specimens. The image resolution was 512 \times 512 and/or 1024 \times 1024 pixels (12 bits, 4096 gray levels) and the images were stored on a hard drive.

Gene expression

Total RNA was prepared from rat anterior pituitaries fixed in RNAlater with RNeasy kit (Qiagen; Hilden, Germany) according to the manufacturer's instructions. The first strand cDNA was then synthesized from the total RNA by reverse transcription using random hexamer primers (Invitrogen Co., Carlsbad, CA, USA) and reverse transcriptase (SuperScript III; Invitrogen Co.). Quantitative reverse transcriptase polymerase chain reaction (qRT-PCR) was conducted using the Taq-Man™ Gene Expression Assay (Applied Biosystems, Foster City, CA, USA). To detect expression of the target gene, the following TaqMan Gene Expression Assay primers and probe mixes (Applied Biosystems) were used: VEGF (*Vegfa*, Assay ID: Rn00582935_m1), VEGFR-2 (*Kdr*, Assay ID: Rn00564986_m1), PTTG (*Pttg1*, Assay ID: Rn00574373_m1), HIF-1 α (*Hif1a*, Assay ID: Rn00577560_m1) and GAPDH (*Gapdh*, Assay ID:

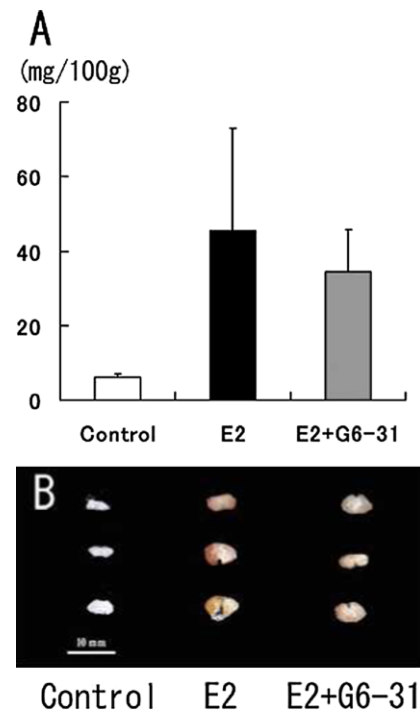


Fig. 2. Pituitary weights and gross findings. Relative pituitary weights were calculated as mg/100g. (A) Tendency to reduction in pituitary weights was seen in the E2+G6-31 group. However there were no significant differences between the E2 and E2+G6-31 groups. The gross features of 3 rats in each group. These pituitaries were immediately fixed in 4% paraformaldehyde solution after sampling. In the E2+G6-31 group, the pituitaries were smaller and their pale color suggested decreased vascularity compared to that in the E2 group.

Rn01462662_g1). Reactions were carried out using the Applied Biosystems 7300 Real-time PCR system and the gene expression levels of the target gene in each sample were determined by the relative quantification method using the GAPDH level as an endogenous control.

Statistical analysis

The results are expressed as means \pm S.D. Comparisons of the individual groups were tested for statistical significance using Student's t-test. All statistical tests were two sided and $P < 0.05$ was considered to be statistically significant.

III. Results

Pituitary weights and Gross findings of E2-induced PRLoma and inhibition by G6-31

After 13 wks of E2 treatment, rat PRLomas developed macroscopically and the relative pituitary weights were significantly increased compared to the pituitaries of the vehicle control group. On the other hand, the relative pituitary weights in the E2+G6-31-group were decreased compare to those of E2 group although the difference between the groups was not statistically significant (Fig. 2A). In the gross findings in the 4% PFA-fixed pituitaries, a diffuse dark reddish appearance was seen in the E2 group (Fig. 2B).

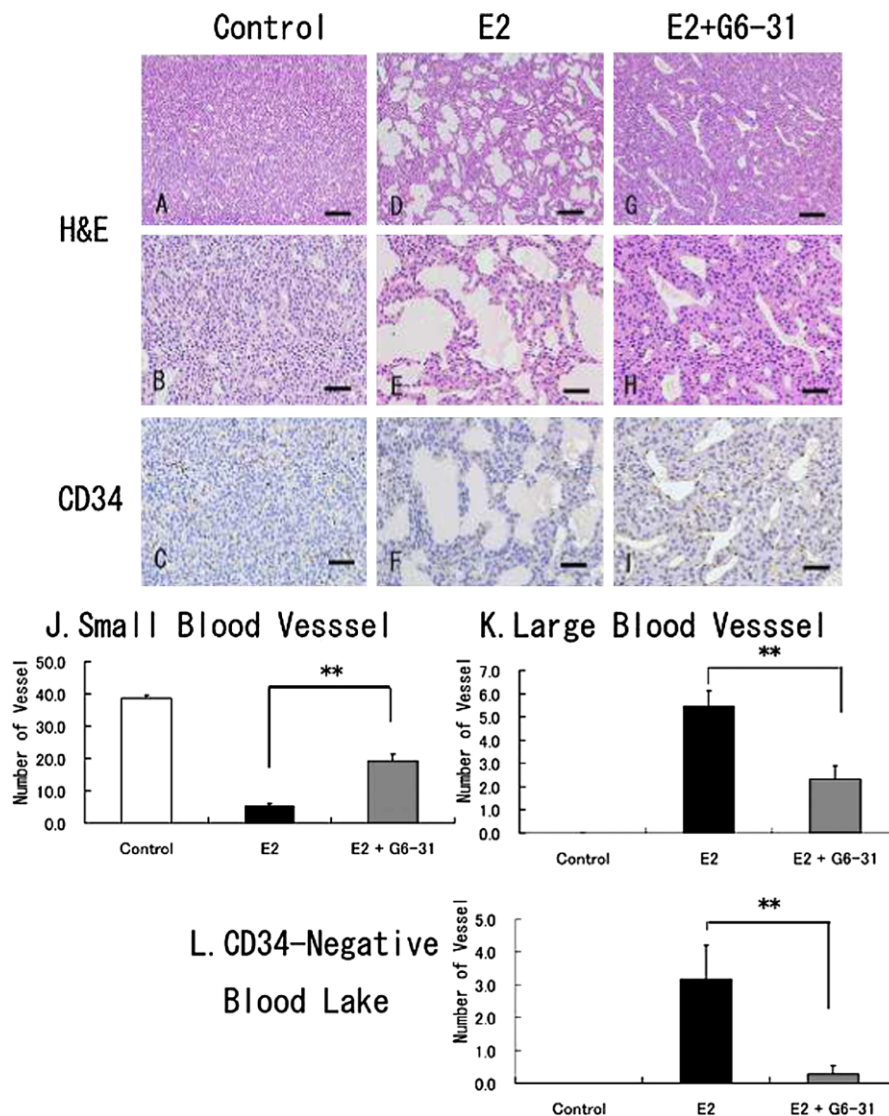


Fig. 3. Histopathological findings for pituitary PRLoma in F344 rats, sectioned stained with H&E (A, B, D, E, G and H) or immunohistochemistry for CD34 as an endothelial marker (C, F and I). Animals in the control group (A to C) or E2 only group (D to F) or E2+G6-31 group (G to I). Distended blood vessels and cystic blood lakes are frequently seen in the E2 induced PRLoma in the E2 group (D to F). Bar=100 μ m (A, D, G) and 50 μ m (B, C, E, F, H and I). J to L: Quantitative examination of the vascular counts in PRLoma; the number of vessels was counted histologically from CD34-stained sections, for small vessels (J), large vessels (K), and CD34-negative blood lakes. **: $P < 0.01$, E2 versus E2+G6-31 group.

However, in the E2+G6-31 group, the pituitaries were smaller and their pale color suggested decreased vascularity compared to that in the E2 group (Fig. 2B).

Histopathology and CD34-positive microvessels

H&E-stained sections of the anterior pituitaries in the E2 group revealed hyperplastic PRL cells and many dilated blood vessels (Fig. 3D and 3E) compared to the features in the control group (Fig. 3A and 3B). In the E2+G6-31 group, hyperplastic PRL cells were decreased in size and the abundance of the dilated blood vessels was primarily diminished with small sized vessels being increased to some extent (Fig. 3G and 3H).

The number of CD34-positive blood vessels was evaluated by microscopic counting. Decrease in the number of CD34-positive small vessels and dilatation of the microvessels were observed in the E2 group as compared to the control group (Fig. 3C and 3F). Moreover, CD34-negative cystic blood lakes not lined by endothelial cells were noticeably increased in the E2 group (Fig. 3F). On the other hand, these findings were observed to be absent after treatment with G6-31 (Fig. 3I). In the CD34 immunohistochemistry, an increase in the number of small blood vessels, and a decrease

in the number of large blood vessels and CD34-negative blood lakes were observed. Significant differences were seen in these findings in the E2+G6-31 group compared with the E2 group (Fig. 3J, 3K, and 3L, **: $P < 0.01$).

Cell proliferation and apoptosis

Examination of cell proliferation in the E2-induced PRLoma showed a marked increase in the number of Ki-67-positive cells in the pituitaries of the rats in the E2 group as compared to the control group (Fig. 4A and 4B). The mean labeling index (LI) of the Ki-67-positive cells was 7.2% in the E2-only treatment *versus* 0.8% in the control group (Fig. 4G). In contrast, a significant decrease in the Ki-67-staining cells was noted in the anterior lobe in the E2+G6-31 group compared to the E2 group (E2+G6-31 group: $3.1 \pm 1.7\%$, $P < 0.05$; Fig. 4C and 4G).

In the observation of apoptotic cells by TUNEL staining, a slight increase in the apoptotic index (AI) in the PRL cells was seen in the E2 group ($0.9 \pm 0.15\%$, Fig. 4E) as compared with the control group ($0.1 \pm 0.08\%$; Fig. 4D and 4H). In the E2+G6-31 group, a significant increase in the AI ($1.3 \pm 0.18\%$) was found as compared to the E2 group ($P < 0.05$; Fig. 4F and 4H).

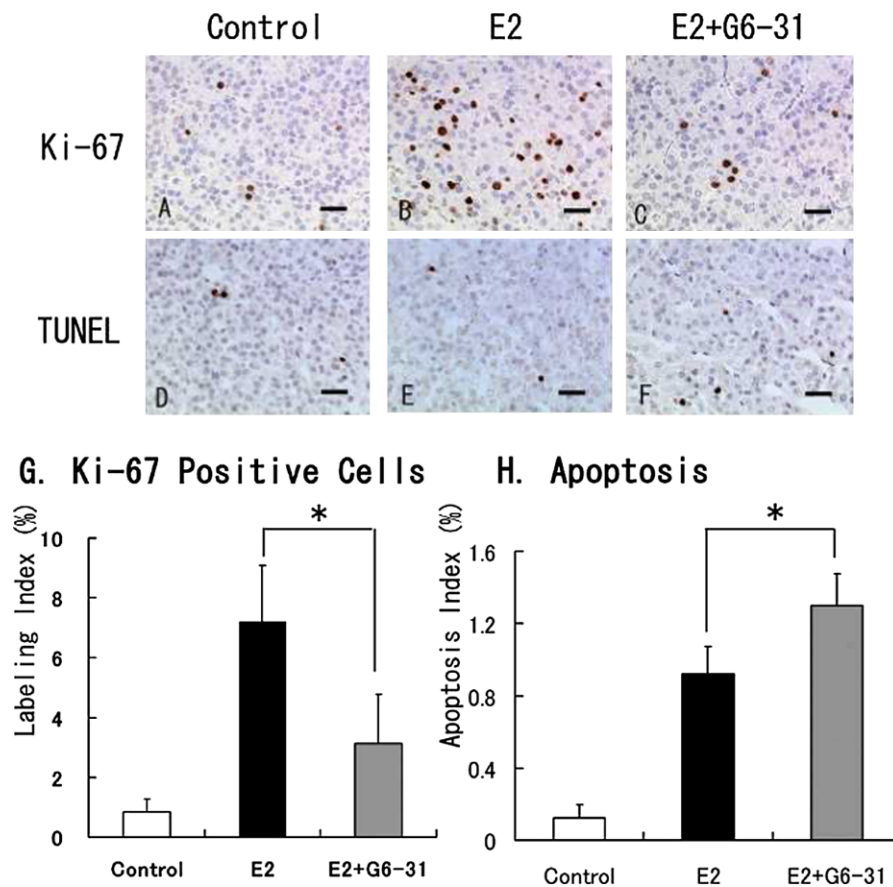


Fig. 4. Tumor cell proliferation and apoptosis in pituitary PRLoma in F344 rats; sections stained with Ki-67 (A to C) or a TUNEL method (D to F). Counterstaining was done with hematoxylin. Bar=50 μ m. **G:** The labeling indexes in the anterior pituitary were calculated from Ki-67 stained sections. **H:** The apoptotic index in the anterior pituitary was also calculated from TUNEL sections. *: $P < 0.05$, E2 versus E2+G6-31 group.

Expression of PRL, VEGF and VEGF-R in the anterior pituitary

After treatment with E2, the PRL-positive cells were diffusely spread in the anterior lobe (Fig. 5A and 5B). In contrast, the intensity of PRL staining and the PRL-positive area was increased in the E2+G6-31 group compared to the E2 group (Fig. 5C). The serum PRL levels, which were determined by radioimmunoassay, showed high levels of serum PRL after the 13 wk treatment with E2 (E2 group: 1843 ± 32 ng/ml) compared to the control group (41 ± 36 ng/ml). In contrast, there was no difference in the PRL concentrations between the E2 and E2+G6-31 groups (E2+G6-31 group: 2250 ± 957 ng/ml).

With immunohistochemistry, VEGF was detected in the cytoplasm of the rat anterior pituitary cells in all groups (Fig. 5D, 5E and 5F), and the VEGF-positive staining area was extended by E2-treatment in both the E2 group and the E2+G6-31 group. The expression of VEGF mRNA was also markedly elevated with treatment with E2. There was no sig-

nificant difference in the intensity of staining and the level of VEGF mRNA expression between the E2+G6-31 group and the E2 group (Fig. 5J).

Immunohistochemistry showed that Flk-1 (VEGFR-2) was diffusely distributed in the anterior pituitary cells and vascular endothelial cells, and its staining was observed faintly in the control group (Fig. 5G). The Flk-1 positive area was increased after treatment with E2, but there was no significant difference in the intensity of the Flk-1 staining in the pituitary cells between the E2 group and the E2+G6-31 group (Fig. 5H and 5I). In addition, Flk-1 positive staining was not noted in the lining of the area of blood lakes observed in the E2 group. On the other hand, the expression level of Flk-1 mRNA was decreased significantly in the E2+G6-31 group compared to the E2 group (Fig. 5K).

Expression of the pituitary tumor transforming gene (PTTG) and HIF-1 α in the anterior pituitary

PTTG localized in the cytoplasm of the anterior pitu-

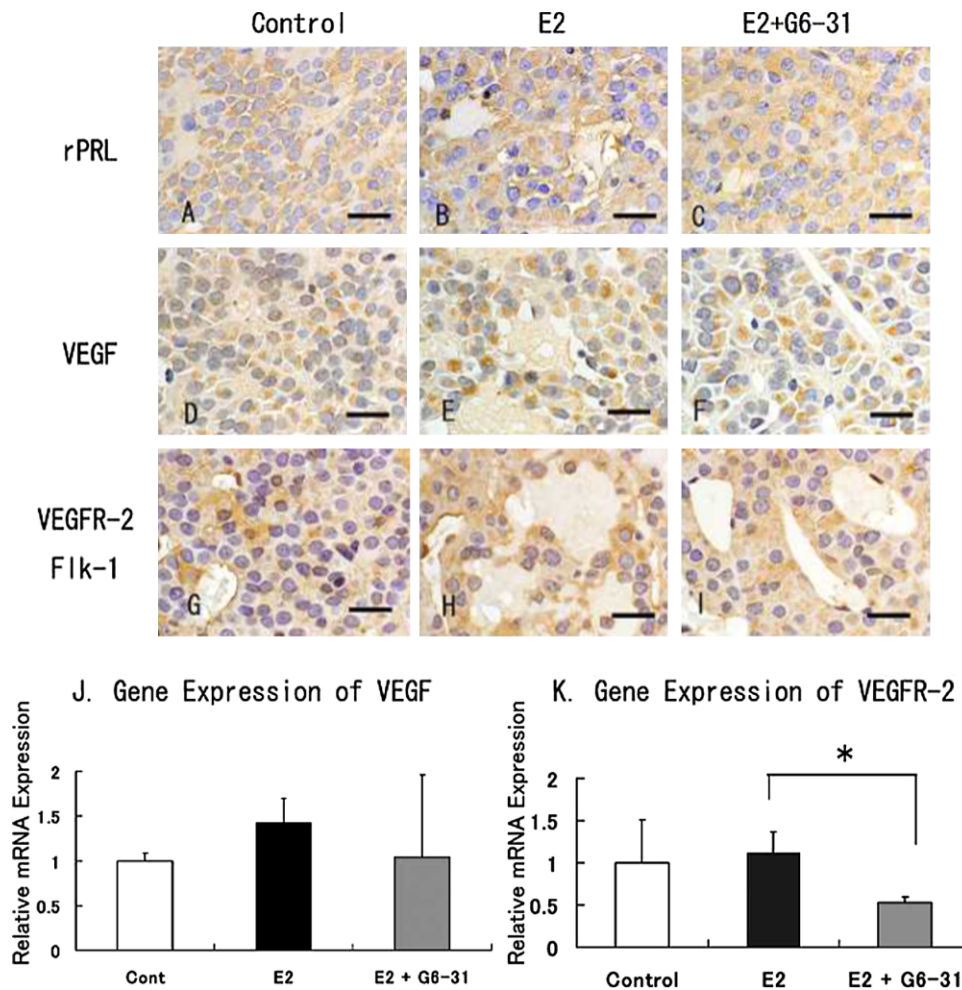


Fig. 5. Immunohistochemistry of pituitary PRLoma in F344 rats. Staining of PRL (A to C), VEGF (D to F), Flk-1 (G to I). Counterstaining was done with hematoxylin. Bar=20 μ m. **J** and **K**: Gene expression of VEGF (**J**) and Flk-1 (**K**) in pituitary PRLoma in F344 rats. The columns show the mean value of the relative expression of VEGF and Flk-1 compared with GAPDH as an endogenous control. *: $P < 0.05$, E2 versus E2+G6-31 group.

itary cells and PTTG-positive cells were increased after treatment with E2 (Fig. 6A and 6B). Similarly with real time qRT-PCR, PTTG1 mRNA levels were also significantly increased in the E2 group (Fig. 6G). On the other hand, in the E2+G6-31 group a decrease in the number of positive cells and weakened staining intensity were observed in the pituitary cells (Fig. 6C). Significant decrease was also observed in the expression levels of PTTG mRNA in the E2+G6-31 group compare to the E2 group (Fig. 6G).

The intensity of staining for HIF-1 α localized in the cytoplasm of the anterior pituitary cells and the numbers of positive staining cells were increased in the E2+G6-31 group compared to the E2 group (Fig. 6E and 6F). However, the expression of HIF-1 α mRNA in the anterior pituitary showed no differences between the groups (Fig. 6H)

3D image analysis of the intra-pituitary microvessels

In 3D image analysis using CLSM, the fine vascular network structure of the anterior pituitary was seen in the control group (Fig. 7A). On the other hand, irregular distension, excessive branching and a segmented pattern and partial loss of vessels were frequently observed in the E2 group (Fig. 7B). Compared to the control group and E2 group, decrease in distended and segmented pattern and focal appearance of fine microvessels in the anterior pituitary were clearly observed in the E2+G6-31 group (Fig. 7C).

IV. Discussion

VEGF is one of the most potent and specific angiogenic factors, and contributes to the growth of many malignant tumors [25], including pituitary adenoma with promoting tumor angiogenesis and angiectasis. The induction of VEGF expression by estrogen has been demonstrated in many target organs and the role of estrogen in endocrine tissue has been suggested as modulation of angiogenesis and vascular permeability [13]. As E2-induced pituitary PRLoma has shown adequate vascularization, it is expected that VEGF contributes to the development of the increased vascularity and resulting increased size of PRLoma [42, 52].

The monoclonal antibody against VEGF, bevacizumab, was approved for treatment of metastatic colorectal and non-small lung cell carcinoma, but the effect of anti-VEGF therapy on endocrine tumors has not been reported in clinical practice. The anti-human and murine VEGF-A monoclonal antibody, G6-31, is expected to be a prospective candidate as an anti-angiogenic agent. In this study, after simultaneous treatment with G6-31, pituitary PRLoma induced by E2 in female F344 rats demonstrated significant reduction in tumor progression. Specifically, G6-31 diminished the E2-induced Ki-67 labeling index of anterior pituitary cells, which were considered to be mainly PRL cells. It also enhanced pituitary cell apoptosis and increased the number

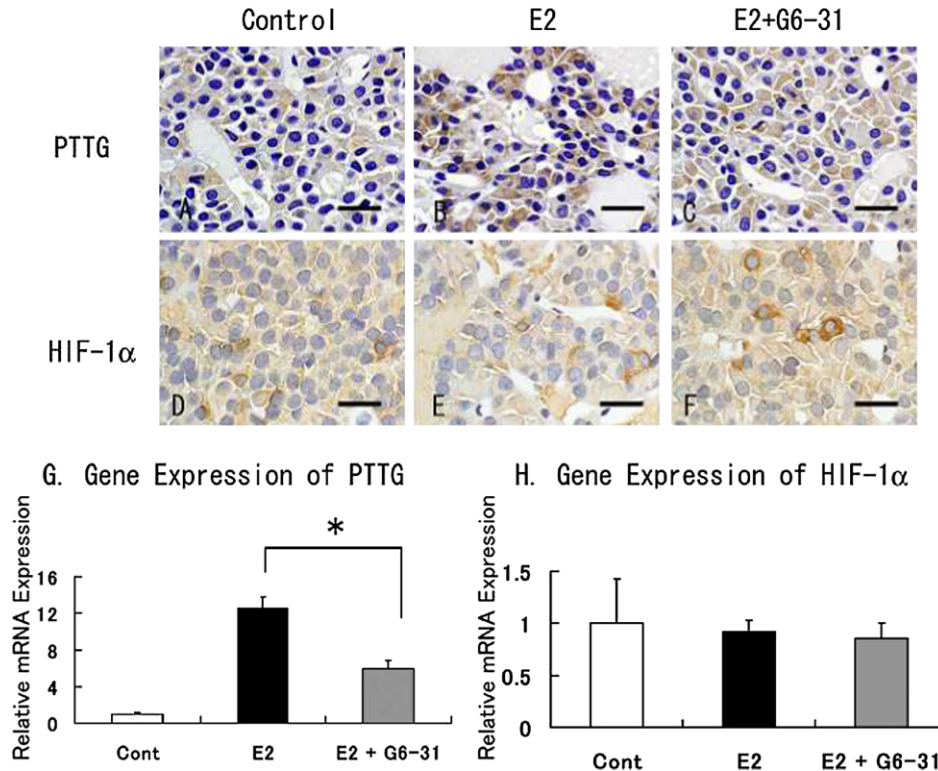


Fig. 6. Immunohistochemistry of pituitary PRLoma in F344 rats. Staining of PTTG (A to C) and HIF-1 α (D to F). Counterstaining was done with hematoxylin. Bar=20 μ m. **G** and **H**: Gene expression of PTTG (**G**) and HIF-1 α (**H**) in pituitary PRLoma in F344 rats. The columns show the mean value of the relative expression of PTTG and HIF-1 α compared with GAPDH as an endogenous control. *: $P < 0.05$, E2 versus E2+G6-31 group.

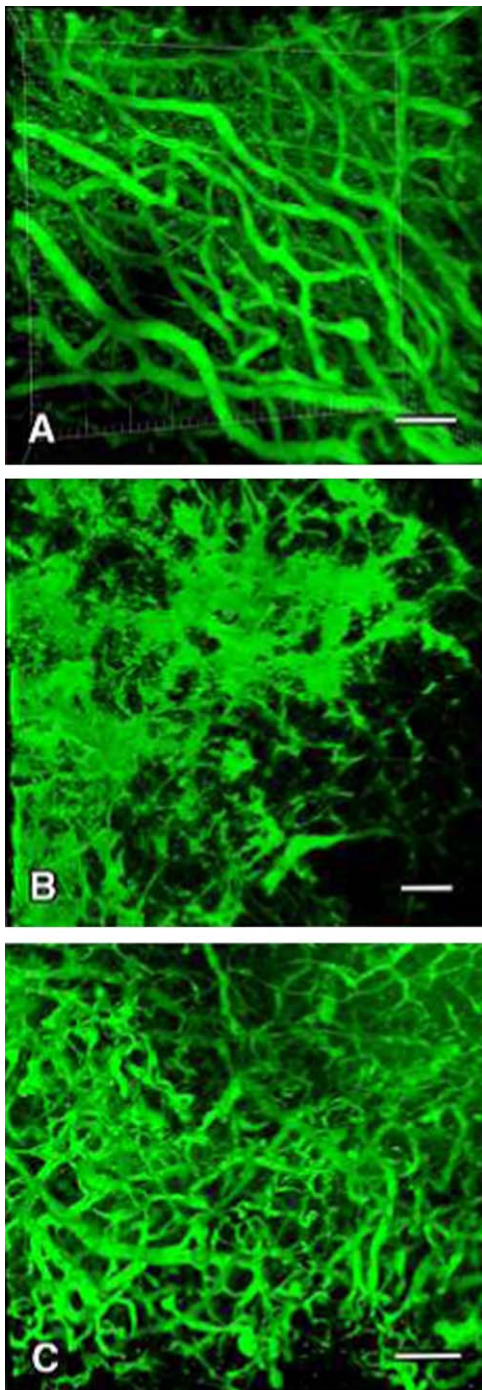


Fig. 7. 3D-image analysis using confocal laser scanning microscopy of the pituitary vessels of PRLoma in F344 rats. Infused FITC-gelatin into the anterior pituitary microvessels was used to show the blood flow in the anterior lobe. These images show the control group (A), E2 group (B), and E2+G6-31 group (C). In the control group, fine vascular network structure of the anterior pituitary was seen (A). On the other hand, in the E2 group irregular distension, excessive branching and a segmented pattern and partial loss of vessels were noted (B). In the E2+G6-31 group, decrease in distended and segmented pattern and focal appearance of fine microvessels in the anterior pituitary were clearly observed compared to the control and E2 group (C).

of microvessels with decreased blood lakes detected by CD34 immunohistochemistry and 3D-imaging analysis of the features of FITC injected microvessels. Blood lakes not lined by CD34-positive endothelial cells were observed in the E2 group and disappeared in the E2+G6-31 group. Moreover, in the endothelial cells of fine vessels in control group and E2+G6-31 group, there was no significant difference in the cell proliferation or the immunohistochemistry findings, for CD34 and Flk-1. These findings were considered to be due to the suppression of angiectasis and vascular permeability by the simultaneous use of G6-31.

These results suggested that VEGF-A blockade by the anti-tumor properties of G6-31 may provide an effective treatment for pituitary tumors in association with anti-proliferative and pro-apoptotic actions as well as anti-angiogenic actions and effects on microvascular permeability.

It has been reported that G6-31 inhibits significant tumor growth and suggested that the mechanism is by inhibited angiogenesis [33] which significantly extends the survival of *Apc^{+/-min}* mice [31]. The data from these studies, together with our data, indicate that the antitumor activity of G-31 is related to its anti-angiogenic action.

The tumor blood vessels in the rat PRLoma are functionally pathological, i.e. their size is variable and they are excessively branched and dilated [27, 28]. In 3-D image analysis FITC-conjugate injected pituitary vessels visualized by CLSM, treatment with G6-31 provides equal prognostic inhibition as bromocriptine, a dopamine agonist, of prolactin production in lactotrophs [10, 26, 29, 35]. Furthermore antiangiogenic agents such as thalidomide [50], and a matrix metalloproteinase inhibitor [41] are reported to inhibit PRLoma growth based on a strategy to block angiogenesis.

An increase in the protein level of HIF-1 α was observed by immunohistochemistry in the pituitaries of E2+G6-31 group. The expression of HIF-1 α has been reported to have a strong correlation with reduced oxygen supply and subsequent apoptosis leading to hypoxia-dependent cell death [5]. The increase in HIF-1 α expression in the cytoplasm (Fig. 6) after treatment with G6-31 is hypoxia-dependent in PRLoma. Under normoxic conditions, HIF-1 α levels are reduced by constant proteosomal degradation, whereas under hypoxic conditions the HIF-1 α protein becomes stabilized. Therefore, strong staining for HIF-1 α by immunohistochemistry represents a useful marker for low-oxygen situations such as the findings in the pituitaries in the E2+G6-31 group, and this finding might be related to the increase in apoptosis in this group. This finding was considered to be related to the pharmacological action of G6-31.

PTTG interacts with the expression of proangiogenic growth factors and tumorigenesis with the angiogenic phenotype of PRLomas [22, 36, 40]. As a homolog of securine PTTG regulates the cell cycle and higher expression of PTTG was noted in pituitary adenomas. Experimentally, PTTG has also been shown to be regulated by exposure to estrogen [23, 39] and our results demonstrated that lowered

Summary of G6-31 Inhibitory effect on development of E2-induced PRLoma

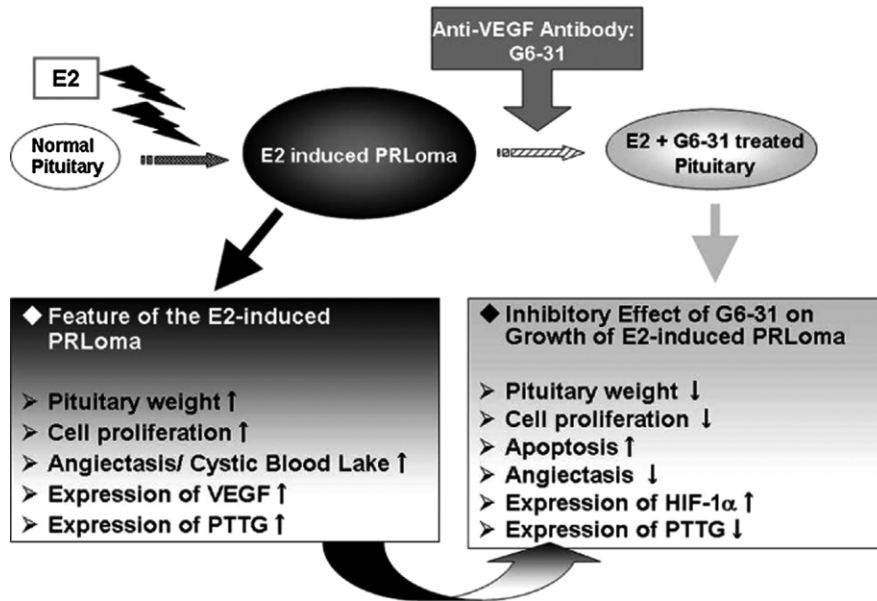


Fig. 8. Schematic illustration of this study: the findings of E2-induced PRLoma were typically observed with the 13-wk treatment in the E2 group in this study and the inhibitory effect were observed in the E2+G6-31 group with simultaneous use of G6-31 (Anti-VEGF-A antibody) for the last 3 wks of the E2 treatment period.

levels of PTTG were observed in the E2+G6-31 group. Thus, this finding suggests that the inhibitory effect of anti-VEGF antibody on estrogen dependent tumor growth includes the inhibition of angiogenesis and the reduction of tumor cell proliferation.

VEGFR-1 (Flt-1) and VEGFR-2 (KDR, /FLK-1) are expressed on the cell surface of most blood endothelial cells, whereas VEGFR-3 is largely restricted to the lymphatic endothelial cells. VEGF-A binds both VEGFR-1 and VEGFR-2, while PlGF and VEGF-B interact only with VEGFR-1. VEGF-C and VEGF-D bind VEGFR-2 and VEGFR-3. Among them, VEGFR-1 and VEGFR-2 are tyrosine kinase receptors that mediate the signal activity of VEGF-A, and of these two, VEGFR-2 is the main receptor mediating most of the endothelial cell mitogenesis, survival, and microvascular permeability [14, 48]. Banerjee *et al.* [2] demonstrated that the expression of VEGF and its receptor, Flk-1 protein, was enhanced significantly in the pituitary after 7 days of treatment with estrogen, and the level of gene expression markedly accelerated during prolonged estrogen exposure. In our study, VEGF and Flk-1 were detected in the anterior pituitary cells by immunohistochemistry and VEGF may function as a growth factor with autocrine/paracrine regulation, so blocking VEGF-A could produce; (1) decrease in the amount of anterior cell proliferation, (2) inhibition of the vascular pathological features including decrease in the cystic blood lakes and distended vessels, (3) improvement in vascular findings in 3D imaging analysis. In addition, since it has been reported that VEGFR-2 stimulation is responsible for the induction of vascular permeability by VEGF [14, 48], these inhibitory findings in the

E2+G6-31 group may be related to suppression of the vascular permeability in E2 induced PRLoma.

In summary, our results demonstrated the effect of G6-31 on anti-angiogenesis and tumor inhibition during the development of estrogen-induced tumor cell proliferation and angiectasis in the anterior pituitary (Fig. 8). The data suggest that this experimental design using E2-induced PRLomas could serve as a model to study the therapeutic effects of anti-VEGF agents on vascular-rich endocrine tumors by the effects proposed by Folkman *et al.* and Folkman [15, 16]. Furthermore, anti-VEGF agents could become a nonsurgical treatment for human vascular-rich endocrine tumors.

V. Acknowledgements

The authors wish to thank Drs. Kenneth Hillan and Napoleone Ferrara, Genentech Inc., for kindly supplying the anti-human and murine VEGF-A monoclonal antibody (G6-31, Lot No. 11037) used in this study. A portion of this study was presented at the Endocrine Society's 89th Annual Meeting on June 4, 2007 in Toronto, Ontario, and the 97th Annual Meeting of United States and Canadian Academy of Pathology on March 1–7, 2008 in Denver, Colorado. The abstract was previously published in *Modern Pathology*, Vol. 21 (Suppl) 108A, 2008.

VI. References

1. Banerjee, S. K., Sarkar, D. K., Weston, A. P., De, A. and Campbell, D. R. (1997) Over expression of vascular endothelial growth factor and its receptor during the development of

- estrogen-induced rat pituitary tumors may mediate estrogen-initiated tumor angiogenesis. *Carcinogenesis* 18; 1155–1161.
2. Banerjee, S. K., Zoubine, M. N., Tran, T. M., Weston, A. P. and Campbell, D. R. (2000) Overexpression of vascular endothelial growth factor164 and its co-receptor neuropilin-1 in estrogen-induced rat pituitary tumors and GH3 rat pituitary tumor cells. *Int. J. Oncol.* 16; 253–260.
 3. Bosari, S., Lee, A. K., DeLellis, R. A., Wiley, B. D., Heatley, G. J. and Silverman, M. L. (1992) Microvessel quantitation and prognosis in invasive breast carcinoma. *Hum. Pathol.* 23; 755–761.
 4. Brem, S., Cotran, R. and Folkman, J. (1972) Tumor angiogenesis: a quantitative method for histologic grading. *J. Natl. Cancer Inst.* 48; 347–356.
 5. Carmeliet, P., Dor, Y., Herbert, J. M., Fukumura, D., Brusselmans, K., Dewerchin, M., Neeman, M., Bono, F., Abramovitch, R., Maxwell, P., Koch, C. J., Ratcliffe, P., Moons, L., Jain, R. K., Collen, D. and Keshert, E. (1998) Role of HIF-1 α in hypoxia-mediated apoptosis, cell proliferation and tumor angiogenesis. *Nature* 394; 485–490.
 6. Cracchiolo, D., Swick, J. W., McKiernan, L., Sloan, E., Raina, S., Sloan, C. and Wendell, D. L. (2002) Estrogen-dependent growth of a rat pituitary tumor involves, but does not require, a high level of vascular endothelial growth factor. *Exp. Biol. Med.* 227; 492–499.
 7. D'Amato, R., Wesolowski, E. and Smith, L. E. (1993) Microscopic visualization of the retina by angiography with high-molecular-weight fluorescein-labeled dextrans in the mouse. *Microvasc. Res.* 46; 135–142.
 8. Egashira, N., Minematsu, T., Miyai, S., Takekoshi, S., Camper, S. A. and Osamura, R. Y. (2005) Pituitary changes in Prop1 transgenic mice: hormone producing tumors and signet-ring type gonadotropes. *Acta Histochem. Cytochem.* 41; 47–57.
 9. Elias, K. A. and Weiner, R. I. (1984) Direct arterial vascularization of estrogen-induced prolactin secreting anterior pituitary tumors. *Proc. Natl. Acad. Sci. U S A* 81; 4549–4553.
 10. Elias, K. A. and Weiner, R. I. (1987) Inhibition of estrogen-induced anterior pituitary enlargement and arteriogenesis by bromocriptine in Fischer 344 rats. *Endocrinology* 120; 617–621.
 11. Ferrara, N. (2000) Vascular endothelial growth factor and the regulation of angiogenesis. *Recent Prog. Horm. Res.* 55; 15–35; discussion 35–6.
 12. Ferrara, N. (2000) VEGF: an update on biological and therapeutic aspects. *Curr. Opin. Biotechnol.* 11; 617–624.
 13. Ferrara, N., Gerber, H. P. and LeCouter, J. (2003) The biology of VEGF and its receptors. *Nat. Med.* 9; 669–676.
 14. Ferrara, N. (2004) Vascular endothelial growth factor: basic science and clinical progress. *Endocr. Rev.* 25; 581–611.
 15. Folkman, J., Merler, E., Abernathy, C. and Williams, G. (1971) Isolation of a tumor factor responsible for angiogenesis. *J. Exp. Med.* 1; 275–288.
 16. Folkman, J. (1995) Angiogenesis inhibitors generated by tumors. *Mol. Med.* 1; 120–122.
 17. Folkman, J. (2004) Endogenous angiogenesis inhibitors. *APMIS.* 112; 496–507.
 18. Fox, S. B. and Harris, A. L. (2004) Histological quantitation of tumour angiogenesis. *APMIS.* 112; 413–430.
 19. Fuh, G., Wu, P., Liang, W. C., Ultsch, M., Lee, C. V., Moffat, B. and Wiesmann, C. (2006) Structure-function studies of two synthetic anti-vascular endothelial growth factor Fabs and comparison with the Avastin Fab. *J. Biol. Chem.* 10; 6625–6631.
 20. Gomez, O. and Balsa, J. A. (2003) Autocrine/paracrine action of pituitary vasoactive intestinal peptide on lactotroph hyperplasia induced by estrogen. *Endocrinology* 144; 4403–4409.
 21. Hanahan, D. and Folkman, J. (1996) Patterns and emerging mechanisms of the angiogenic switch during tumorigenesis. *Cell* 86; 353–364.
 22. Heaney, A. P. and Melmed, S. (1999) Pituitary tumour transforming gene: a novel factor in pituitary tumour formation. *Baillieres Best Pract. Res. Clin. Endocrinol. Metab.* 13; 367–380.
 23. Heaney, A. P., Horwitz, G. A., Wang, Z., Singson, R. and Melmed, S. (1999) Early involvement of estrogen-induced pituitary tumor transforming gene and fibroblast growth factor expression in prolactinoma pathogenesis. *Nat. Med.* 5; 1317–1321.
 24. Henderson, B. E., Ross, R. and Bernstein, L. (1988) Estrogens as a cause of human cancer: the Richard and Hinda Rosenthal Foundation Award lecture. *Cancer Res.* 48; 246–253.
 25. Hyder, S. M., Nawaz, Z., Chiappetta, C. and Stancel, G. M. (2000) Identification of functional estrogen response elements in the gene coding for the potent angiogenic factor vascular endothelial growth factor. *Cancer Res.* 60; 3183–3190.
 26. Itoh, J., Kawai, K., Serizawa, A., Yamamoto, Y., Ogawa, K., Matsuno, A., Watanabe, K. and Osamura, R. Y. (2001) Three-dimensional imaging of hormone-secreting cells and their microvessel environment in estrogen-induced prolactinoma of the rat pituitary gland by confocal laser scanning microscopy. *Appl. Immunohistochem. Mol. Morphol.* 9; 364–370.
 27. Jakubowski, J. (1995) Blood supply, blood flow and autoregulation in the adenohypophysis, and altered patterns in oestrogen induced adenomatous hyperplasia. *Br. J. Neurosurg.* 9; 331–346.
 28. Jugenburg, M., Kovacs, K., Stefaneanu, L. and Scheithauer, B. W. (1995) Vasculature in nontumorous hypophyses, pituitary adenomas, and carcinomas: a quantitative morphologic study. *Endocr. Pathol.* 6; 115–124.
 29. Kemeny, A. A., Jakubowski, J., Stawowy, A., Smith, C. and Timperley, W. R. (1987) Changes of blood flow in oestrogen-induced hyperplastic anterior pituitary lobe following bromocriptine administration. *Br. J. Neurosurg.* 1; 243–250.
 30. Komorowski, J., Jankewicz, J. and Stepień, H. (2000) Vascular endothelial growth factor (VEGF), basic fibroblast growth factor (bFGF) and soluble interleukin-2 receptor (sIL-2R) concentrations in peripheral blood as markers of pituitary tumours. *Cytobios* 101; 151–159.
 31. Korsisaari, N., Kasman, I. M., Forrest, W. F., Pal, N., Bai, W., Fuh, G., Peale, F. V., Smits, R. and Ferrara, N. (2007) Inhibition of VEGF-A prevents the angiogenic switch and results in increased survival of Apc+/min mice. *Proc. Natl. Acad. Sci. U S A* 19; 10625–10630.
 32. Korsisaari, N., Ross, J., Wu, X., Kowanetz, M., Pal, N., Hall, L., Eastham-Anderson, J., Forrest, W. F., Van Bruggen, N., Peale, F. V. and Ferrara, N. (2008) Blocking vascular endothelial growth factor-A inhibits the growth of pituitary adenomas and lowers serum prolactin level in a mouse model of multiple endocrine neoplasia type 1. *Clin. Cancer Res.* 1; 249–258.
 33. Liang, W. C., Wu, X., Peale, F. V., Lee, C. V., Meng, Y. G., Gutierrez, J., Fu, L., Malik, A. K., Gerber, H. P., Ferrara, N. and Fuh, G. (2006) Cross-species vascular endothelial growth factor (VEGF)-blocking antibodies completely inhibit the growth of human tumor xenografts and measure the contribution of stromal VEGF. *J. Biol. Chem.* 13; 951–961.
 34. Lloyd, R. V. (1983) Estrogen-induced hyperplasia and neoplasia in the rat anterior pituitary gland. An immunohistochemical study. *Am. J. Pathol.* 113; 198–206.
 35. Matsuno, A., Takekoshi, S., Sanno, N., Utsunomiya, H., Ohsugi, Y., Saito, N., Kanemitsu, H., Tamura, A., Nagashima, T., Osamura, R. Y. and Watanabe, K. (1997) Modulation of protein kinases and microtubule-associated proteins and changes in ultrastructure in female rat pituitary cells: effects of estrogen and bromocriptine. *J. Histochem. Cytochem.* 45; 805–813.
 36. McCabe, C. J., Boelaert, K., Tannahill, L. A., Heaney, A. P., Stratford, A. L., Khaira, J. S., Hussain, S., Sheppard, M. C., Franklyn, J. A. and Gittoes, N. J. (2002) Vascular endothelial growth factor, its receptor KDR/Flk-1, and pituitary tumor trans-

- forming gene in pituitary tumors. *J. Clin. Endocrinol. Metab.* 87; 4238–4244.
37. Melmed, S. (2003) Mechanisms for pituitary tumorigenesis: the plastic pituitary. *J. Clin. Invest.* 112; 1603–1618.
 38. Millauer, B., Longhi, M. P., Plate, K. H., Shawver, L. K., Risau, W., Ullrich, A. and Strawn, L. M. (1996) Dominant-negative inhibition of Flk-1 suppresses the growth of many tumor types in vivo. *Cancer Res.* 56; 1615–1620.
 39. Minematsu, T., Miyai, S., Suzuki, M., Yamazaki, M., Takekoshi, S. and Osamura, R. Y. (2005) Molecular and histological studies of pituitary tumorigenesis using experimental animal models. *Acta Histochem. Cytochem.* 38; 87–92.
 40. Minematsu, T., Suzuki, M., Sanno, N., Takekoshi, S., Teramoto, A. and Osamura, R. Y. (2006) PTTG overexpression is correlated with angiogenesis in human pituitary adenomas. *Endocr. Pathol.* 17; 143–153.
 41. Mucha, S. A., Meleń-Mucha, G., Godlewski, A. and Stepień, H. (2007) Inhibition of estrogen-induced pituitary tumor growth and angiogenesis in Fischer 344 rats by the matrix metalloproteinase inhibitor batimastat. *Virchows Arch.* 450; 335–341.
 42. Ochoa, A. L., Mitchner, N. A., Paynter, C. D., Morris, R. E. and Ben-Jonathan, N. (2000) Vascular endothelial growth factor in the rat pituitary: differential distribution and regulation by estrogen. *J. Endocrinol.* 165; 483–492.
 43. Onofri, C., Carbia Nagashima, A., Schaaf, L., Feirer, M., Lohrer, P., Stummer, W., Berner, S., Chervin, A., Goldberg, V., Stalla, G. K., Renner, U. and Arzt, E. (2004) Estradiol stimulates vascular endothelial growth factor and interleukin-6 in human lactotroph and lactosomatotroph pituitary adenomas. *Exp. Clin. Endocrinol. Diabetes.* 112; 18–23.
 44. Osamura, R. Y. and Watanabe, K. (1986) Ultrastructural localization of prolactin in estrogen-induced prolactinoma of the rat pituitary. Experimental models for the human prolactinomas and the effects of bromocriptine. *Acta Pathol. Jpn.* 36; 1131–1137.
 45. Osamura, R. Y., Egashira, N., Kajiya, H., Takei, M., Tobita, M., Miyakoshi, T., Inomoto, C., Takekoshi, S. and Teramoto, A. (2009) Pathology, pathogenesis and therapy of growth hormone (GH)-producing pituitary adenomas: Technical advances in histochemistry and their contribution. *Acta Histochem. Cytochem.* 42; 95–104.
 46. Persson, I. (2000) Estrogens in the causation of breast, endometrial and ovarian cancers—evidence and hypotheses from epidemiological findings. *J. Steroid Biochem. Mol. Biol.* 74; 357–364.
 47. Phelps, C. and Hymer, W. C. (1983) Characterization of estrogen-induced adenohypophyseal tumors in the Fischer 344 rat. *Neuroendocrinology* 37; 23–31.
 48. Shibuya, M. and Claesson-Welsh, L. (2006) Signal transduction by VEGF receptors in regulation of angiogenesis and lymphangiogenesis. *Exp. Cell Res.* 312; 549–560.
 49. Stepień, H. M., Kolomecki, K., Pasięka, Z., Komorowski, J., Stepień, T. and Kuzdak, K. (2002) Angiogenesis of endocrine gland tumours—new molecular targets in diagnostics and therapy. *Eur. J. Endocrinol.* 146; 143–151.
 50. Stepień, H., Lawnicka, H., Mucha, S., Wagrowska-Danilewicz, M., Stepień, B., Siejka, A. and Komorowski, J. (2006) Inhibitory effect of thalidomide on the growth, secretory function and angiogenesis of estrogen-induced prolactinoma in Fischer 344 rats. *Life Sci.* 79; 1741–1748.
 51. Strottmann, J. M., Robinson, J. B. Jr. and Stellwagen, E. (1983) Advantages of preelectrophoretic conjugation of polypeptides with fluorescent dyes. *Anal. Biochem.* 132; 334–337.
 52. Takada, K., Yamada, S. and Teramoto, A. (2004) Correlation between tumor vascularity and clinical findings in patients with pituitary adenomas. *Endocr. Pathol.* 15; 131–139.
 53. Vidal, S., Lloyd, R. V., Moya, L., Scheithauer, B. W. and Kovacs, K. (2002) Expression and distribution of vascular endothelial growth factor receptor Flk-1 in the rat pituitary. *J. Histochem. Cytochem.* 50; 533–540.
 54. Waltenberger, J., Claesson-Welsh, L., Siegbahn, A., Shibuya, M. and Heldin, C. H. (1994) Different signal transduction properties of KDR and Flt1, two receptors for vascular endothelial growth factor. *J. Biol. Chem.* 269; 26988–26995.

This is an open access article distributed under the Creative Commons Attribution License, which permits unrestricted use, distribution, and reproduction in any medium, provided the original work is properly cited.
